Available online at https://ifejost.oauife.edu.ng

IFE JOURNAL OF SCIENCE AND TECHNOLOGY

Vol 8. No. 1 (2024) 58 – 74

Theoretical evaluation of the photovoltaic performance of some porphyrinoid compounds as potential sensitizers in DSSCs

Sanusi, K.* **and Fatomi, N. O.**
Department of Chemistry, Obafemi Awolowo University, Ile-Ife, Nigeria
*Corresponding Author's Email: sosanusi@oauife.edu.ng
Tel: +234-903-116-7556, +234-705-067-9851

Abstract

This study investigates the effects of substituents and solvents on the photovoltaic properties of some selected porphyrinoid systems for application in dye-sensitized solar cells (DSSCs). Their photophysical and photovoltaic properties were studied in vacuum, acetonitrile (AcCN), dichloromethane (DCM), dimethyl sulfoxide (DMSO), and ethanol (EtOH) for possible application as sensitizers in DSSCs. Electronic absorption properties of the porphyrinoids were obtained via potential energy surface scan (PESs) calculations and TD-DFT, while their thermodynamic properties were obtained by DFT in the selected media. A total of twenty-one compounds were generated by replacing one or all the original substituents in a porphyrinoid with -CO_2H. The best performing sensitizers judging by their incident-photon conversion (IPCE) values were found to be Por2 (6.85×10^{-11}) and Pht7 (6.63×10^{-11}) with AcCN as the solvent. The compounds did not show considerable fascinating photovoltaic performance in the other solvents (DCM, DMSO and EtOH). Overall, the study predicts that Por2 and Pht7 are the best sensitizers among those investigated. It also shows the enduring property of AcCN as the most suitable solvent for photovoltaic activity.

Keywords: Porphyrins, phthalocyanines, fluorescence factor, electronic excited state

---

INTRODUCTION

One of the significant challenges the world is currently facing is the rise in global energy demands and concurrent increase in air pollution with attendant effects of climate change (Carella *et al*., 2018). A recent International Energy Agency (IEA) (International Energy Agency, 2020) report has projected that the world energy consumption would increase by 25% by the year 2040. This is expected to increase fossil fuels consumption further rapidly, being a global primary energy source. The implication of this is that the rate of environmental pollution from this activity will also increase. To minimize this effect, attempts to invent sustainable and affordable cleaner energy-producing technologies are being made (Carella *et al*., 2018). Among these technologies are the solar cell devices, which can generate electric power by directly harnessing solar energy. The research in solar cell devices has garnered intense attention over the last three decades, especially the type that uses organic dyes as its source of photosensitization (Carella *et al*., 2018). Photovoltaics (PVs) is the collective name for solar cells. The device can convert light (photon) energy into electricity. They are composed of photoelectric materials that can release electrons into an external circuit (Sanusi *et al*., 2023). This effect causes them to absorb photons of light and generate an electron-hole pair, which can be directed to two different contacts connected by a circuit, thus establishing an electric potential difference (Ellis, 2014). PV technology has experienced remarkable growth in recent years owing to its significant cost reduction when compared to other electrical power sources. The power conversion efficiency (PCE) of PV devices made of highly crystalline silicon has been reported to be around 26.7% (Green *et al*., 2018), which is not far from the theoretically possible limit of 31% for the same device (Shockley and Queisser, 1961). Ninety-three percent of all PV-plant devices are silicon-based, thus dominating the PV market (Green *et al*., 2018). It is worthy of note that the high-purity silicon needed for solar cell fabrication can only be produced via highly expensive high-temperature and high-vacuum techniques (Carella *et al*., 2018). Therefore, despite the great potential for clean energy production that solar photovoltaic (PV) cells hold, their widespread adoption is impeded by the steep production costs, material availability, and complexity in production steps (Desai and Nelson, 2017). Also, silicon-based solar cells are known to have short life span due to the rapid recombination of holes and electrons generated during photoexcitation (Carella *et al*., 2018). As a result of these limitations, alternative PV technologies that rely on cheap processes and materials are being developed.

One of the most promising PV technologies is dye-sensitized solar cells (DSSCs), which possess the potential to overcome the challenge of cost and offer a unique advantage over conventional silicon-based solar cells on the aspect of simplicity (Carella *et al*., 2018). DSSCs are thin-film solar cells that are based on the concept of sensitized photoelectrochemical cells proposed by Gerischer in 1968 and developed by O'Regan and Grätzel in 1991. The device relies on light absorption by a sensitizer (dye), which injects an electron into a semiconductor material (typically TiO_2) to generate electrical current. DSSCs consist of a photoanode, a counter electrode, and an electrolyte (Pashaei *et al*., 2015; Mohamed *et al*., 2021). The photoanode is composed of a transparent conductive oxide (TCO) as substrate, a mesoporous layer of metal oxide nanoparticles (usually TiO_2), and a molecular dye responsible for light absorption and electron injection into the conduction band of the metal oxide (Mehmood *et al*., 2014). The counter electrode is usually a platinum-coated substrate that catalyzes the electrolyte reduction. The electrolyte is a solution of redox species (usually iodide/triiodide) that regenerates the oxidized dye and completes the circuit. The DSSC has the potential to provide the much-needed comparatively higher power conversion efficiency with the cheapest material cost and lesser waste volume than silicon-based solar cells (Spinelli *et al*., 2023). They can operate under low-light or diffuse-light conditions (Devadiga *et al*., 2021) and are a cheaper and more environmentally friendly alternative to silicon-based solar cells. Their performance is however affected by the relatively lower PCE they produce, thus limiting their commercialization (Spinelli *et al*., 2023). They also have poor long-term stability due to photothermal degradation of the dye and/or the electrolyte which can be improved by incorporating a suitable central metal (Xu *et al*., 2023).

The performance of DSSCs depends largely on the choice of the dye, which should have high light-harvesting efficiency, good electron injection ability, strong anchoring group, and suitable energy levels (Kaliramna *et al*., 2022). The use of porphyrinoids as sensitizers have attracted attention due to their intense absorption in the visible and near-infrared region, high photothermal stability, high electron injection efficiency, and the ease at which their optical and electronic properties can be fine-tuned by peripheral and axial substitutions (Wang *et al*., 2014). All these properties which have been exhibited by this class of molecules are expected to improve the PCE of DSSCs and increase their photothermal stability. The most common types of porphyrinoids used as sensitizers in DSSCs are porphyrins and Pcs. The two are often used because of the similarity in their structures to that of natural chlorophylls, which are critical components that must be present in green plants for photosynthesis to occur. Photosynthesis has been widely believed to be the process that the whole idea of DSSC mimicked (Matsuo *et al*., 2020). Both class of molecules (porphyrins and phthalocyanines, Figure 1) are intensely colored planar macrocycles with high chemical, thermal, and light stability, which are important requirements for practical photovoltaic applications (Wang *et al*., 2014). Porphyrins have a cyclic structure comprising four pyrrole rings and may also have a central metal ion (Lu *et al*., 2018). The one depicted in Figure 1A is a metal-free porphyrin. In contrast, Pcs have a similar structure, but the four pyrrole rings are replaced by four indoline units (Figure 1B). Pcs can also be metallated (i.e., have a metal center) or be metal-free like the one depicted in Figure 1B (Sanusi *et al*., 2013).

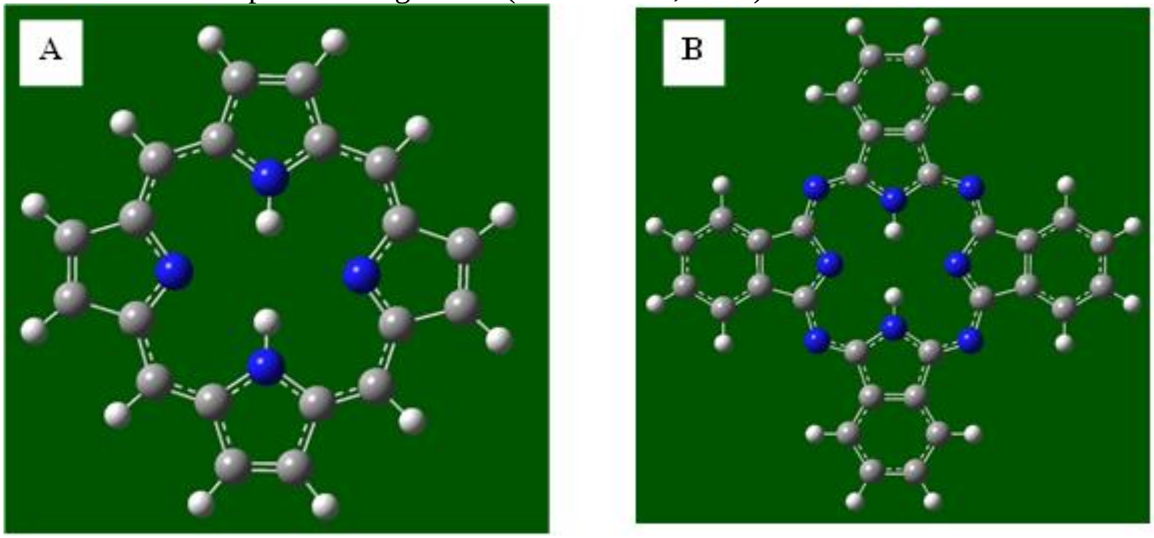

Figure 1: The simplest (A) porphyrin and (B) phthalocyanine molecules.

The adsorption and photovoltaic properties of porphyrinoid compounds can be influenced by the axial, peripheral and the non-peripheral substituent groups on the macrocycle (Sanusi *et al*., 2013; Sanusi *et al*., 2014a; 2014b). These groups can affect the dyes' solubility, aggregation level, energy levels, and electron injection properties (Singh *et al*., 2023). The surrounding solvent can also significantly influence their performance based on their level of solubility in this solvent and its interaction with the mesoporous TiO_2 used as the semiconductor (Labella and Torres, 2023). Moreover, solvents can modulate the binding strength of the dye to the TiO_2 surface, which in turn affects the electron injection efficiency and the overall performance of the cell (Kadish *et al*., 2019).

This study investigated, using density functional theory (DFT) and time-dependent DFT (TD-DFT) methods, the effects of the structure of some selected porphyrinoid compounds on their photovoltaic properties in vacuum and in some selected solvent media. The solvents selected, acetonitrile (AcCN), dichloromethane (DCM), dimethyl sulfoxide (DMSO) and ethanol (EtOH) are common polar organic solvents that are frequently used in the laboratory fabrication and analysis of DSSCs (Sanusi *et al*., 2023). The electronic properties of the selected porphyrinoid compounds were obtained in the presence of the given solvent molecules by computational DFT/TD-DFT methods. These set of solvents were chosen because some of them like the AcCN and DCM represent the most practically used solvents in DSSC research (Sanusi *et al*., 2023; Tontapha *et al*., 2017), and these two have also been previously identified as the most suitable solvents to achieve improved photovoltaic activities (Sanusi *et al*., 2023). EtOH on the other hand was chosen because it is readily available and is one of the most common organic solvents. We chose DMSO because it is a versatile suitable solvent for dissolving “stubborn” organic compounds (i.e., compounds that hardly dissolve in most common organic solvents).

Porphyrins that exhibit some degree of crowding around their *meso*-aryl fragments, at positions 2, 4 and 6, were purposely selected. This expectedly would cause aggregation to be minimized, since aggregation is a known fluorescence quencher (Andrade *et al*., 2008; Ding *et al*., 2021; Safar-Sajadi *et al*., 2021). Previous studies however, had given little or no consideration to aggregation lowering when designing the molecules (Sanusi *et al*., 2019; Sanusi *et al*., 2023). The Pcs on the other hand were selected from literature based on the reports of their solubility in water and common organic solvents (Li *et al*., 2008; Liu *et al*., 2005). Highly soluble Pc molecules are important for efficient photovoltaic activity (Urbani *et al*., 2019). The solubility in these molecules is guaranteed by the pyridinium component in their molecular framework (Urbani *et al*., 2019).

METHODOLOGY

A Gaussian 16 program suite was employed on a peta-scale supercomputing cluster to perform all the calculations (Yilmaz *et al*., 2022). The input files and the results of the calculations were prepared and viewed on GaussView 6.0 visualization software (Sanusi *et al*., 2023). Density functional theory (DFT) and the B3LYP hybrid exchange and correlational functional were used to fully optimize the ground-state geometries of the investigated molecules without imposing any symmetry constraints. The 6-31G(d) basis set was used to carry out these optimizations and GENECP keywords (effective core potential (ECP)) with lanl2dz basis were employed where there is a metal or heavy atom like iodine. The optimized structures were subjected to vibrational frequency calculations at the same level of theories. This step was undertaken to validate the presence of local minima, which represent the lowest points on the potential energy surface, and to determine the corresponding thermodynamic parameters (Thanthiriwatte and de Silva, 2002). Initial optimization and frequency calculations were performed *in vacuo*. The solvent effect was then examined in four different solvents; viz: acetonitrile (AcCN), dimethyl sulfoxide (DMSO), dichloromethane (DCM), and ethanol (EtOH) using the integral equation formalism polarizable continuum solvent model (IEFPCM) (Tomasi *et al*., 2005). The lowest unoccupied molecular orbital (E_{LUMO}), the highest occupied molecular orbital (E_{HOMO}), and the bandgap energies were estimated from the results of the DFT calculations for both the Pcs and porphyrins. The time-dependent DFT (TD-DFT) method was used to perform the relaxed Potential Energy Surface (PES) scan for some of the porphyrins (i.e. those with *meso*-aryl substituents) Figure 2A. Barrier to rotation was imposed around the substituent (*meso*-aryl) angle in the optimized porphyrin structures by constraining the *meso*-aryl dihedral angle in 90° increments and rotating through to a full 360°. This results in 4 distinct steps plus the starting geometry (0°) making 5 steps (0°, 90°, 180°, 270° and 360°). However, for the porphyrins without aryl substituents and all the Pcs (Figure 2B), no dihedral angles were constrained, and the electronic excited state properties (for up to 50 electronic states) of the optimized molecules in the selected media were obtained using the IEF-PCM/TD-B3LYP/6-31G(d) method. The low barrier to rotation imposed during the relaxed PES scans allowed each of the optimized molecules to exist at five different molecular conformations at room temperature, to produce five unique absorption spectral patterns for the molecule, with each at 0°, 90°, 180°, 270°, and 360° orientations (High *et al*., 2015). The dihedral angle constraint was done to mimic the multidimensional motion of molecules when in solution and are exposed to light of varying energies during experimental electronic absorption spectral measurements using UV-visible spectrophotometer. The five conformational absorption spectra were then convolved using MATLAB to obtain one cumulative spectrum for each of the individual porphyrin molecules in the selected media. Key photovoltaic parameters such as light-harvesting efficiency (LHE), electron injection efficiency $\left(\Phi_{\text{inj}} = \phi_f\right)$ and charge collection efficiency (η_c) were estimated from the computed electronic absorption spectral data using the literature method (Sanusi *et al.*, 2023; Sanusi *et al.*, 2020; Balanay and Kim 2008). These properties are closely tied to the incident photon conversion efficiency (IPCE) and are crucial in shedding light on the overall photoelectric behavior of the dyes (Sanusi *et al.*, 2023; Sanusi *et al.*, 2020; Balanay and Kim, 2008).

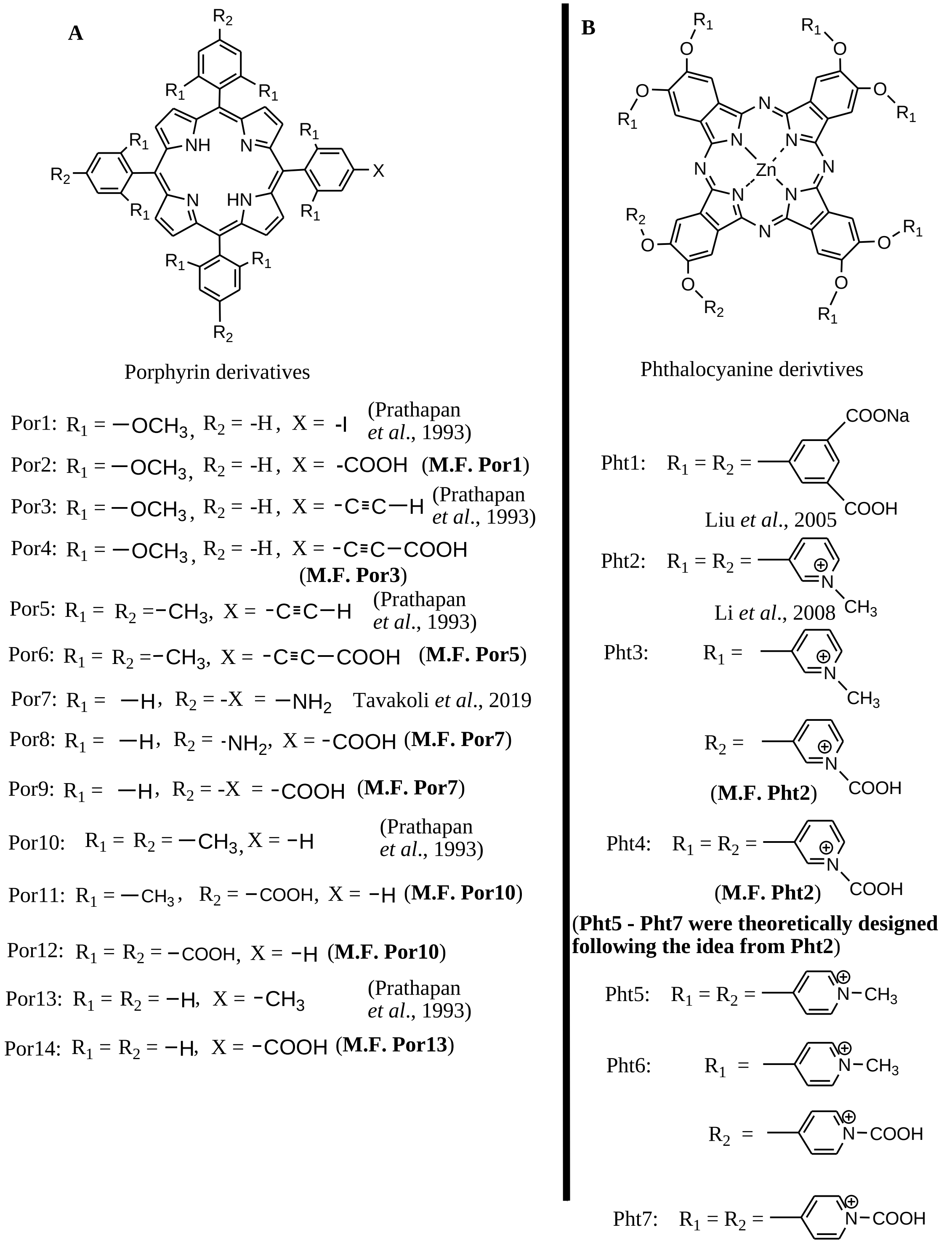

Figure 2: 2-D structures of the investigated molecules. Por1, Por3, Por5, Por7, Por10, Por13, Pht1 and Pht2 are original molecules selected from the refs. (Prathapan *et al.*, 1993),

(Tavakoli *et al*., 2019), (Li *et al*., 2008; Liu *et al*., 2005) accordingly, while the others are modifications from the original molecules as indicated in the figure. The acronym "M.F." represents "modified from".

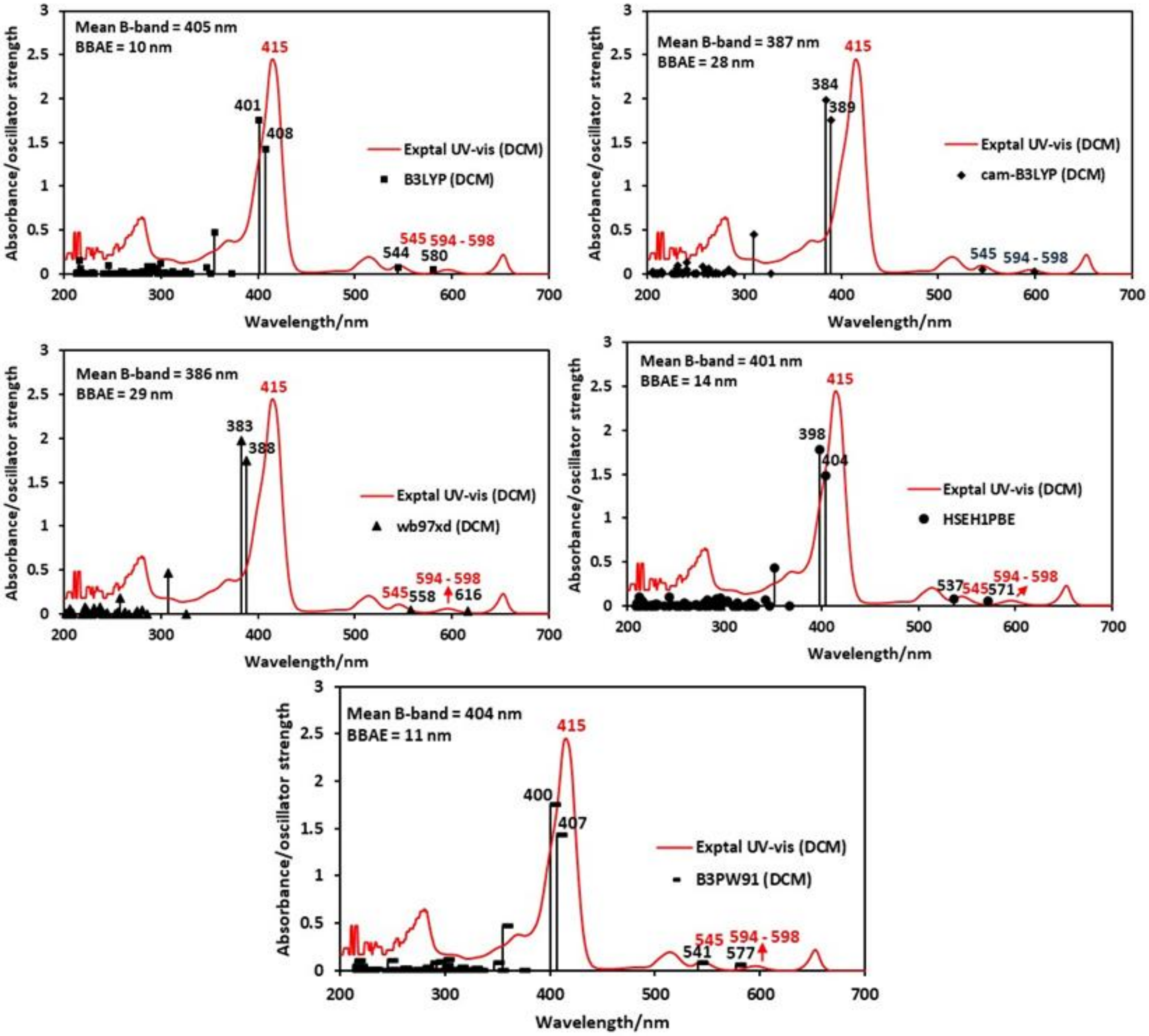

Figure 3: Experimental (red) and calculated (vertical line) electronic absorption spectra of *meso*-tetraphenylporphyrin dichloromethane (DCM). The computed spectra were obtained using five different functionals (B3LYP, CAM-B3LYP, WB97XD, HSEH1PBE and B3PW91) with 6-31G(D) basis set for the purpose of benchmarking. The most significant fingerprint bands are indicated on the spectra. The mean B-band and the B-band absolute error (BBAE) for each method are printed accordingly in the plot areas.

RESULTS AND DISCUSSION

Benchmarking analysis on five different functionals, B3LYP, CAM-B3LYP, WB97XD, HSEH1PBE and B3PW91, was carried out to determine their level of accuracy in predicting the electronic absorption spectra of porphyrinoids using *meso*-tetraphenylporphyrin as sample (Figure 3). All the five functionals predicted only two of the expected four Q-bands for a free-base porphyrin at varying degree of accuracy. Although the B-bands were fully predicted by all the five functionals, the accuracy of these predictions are also at varying degrees. B-band absolute error (BBAE) was obtained by finding the difference between the experimental and computed B-bands to estimate the degree of accuracy of each method. CAM-B3LYP method showed almost a hundred percent accuracy for the two Q-bands predicted out of four, but its BBAE is too wide (28 nm) to be ignored. WB97XD and HSEH1PBE on the other hand have wide deviations in both their B- and Q- bands compared with the experiment (Figure 3). Only B3PW91 showed similar BBAE to B3LYP, but it however showed a higher Q-band deviation from experiment relative to B3LYP. The BBAE obtained for B3LYP was the least among the five functional investigated. The Q-band it predicted are the second most accurate after CAM-B3LYP, when compared its predicted spectra to the experiment with about 1 nm and 16 nm error margin, hence, was considered the best functional at reproducing the experimental UV-vis spectra of porphyrinoids.

The structural modifications of the selected molecules were carried out by changing one or more of the original substituents to -CO_2H group. This is because carboxylic acid group is believed to provide efficient electron transport from dye to TiO_2 semiconductor, and as a result has become a popular anchor group in dyes for DSSC application (Sanusi *et al.*, 2023; Sanusi *et al.*, 2019; Sanusi *et al.*, 2023).

For the porphyrins with *meso*-aryl substitution, the light harvesting efficiency (LHE) was computed by averaging the sum of the oscillator strengths (f_i) within the wavelength range of 200 – 800 nm for each molecular conformation generated during the relaxed scans, f_θ, where θ = 0°, 90°, 180°, 270°, 360°, and then averaging the total sum of f_θ, according to Equation (1):

$$LHE = 1 - 10^{-\Sigma_{\theta=1}^{5} f_\theta /5} \qquad (1)$$

for five geometrical conformations, where $\theta_1 = 0^o,\ \theta_2 = 90^o,\ \theta_3 = 180^o, \theta_4 = 270^o, \theta_5 = 360^o, f_\theta = \frac{\Sigma f_i}{N}$, N = number of oscillator strength within the wavelength range, f_i represents the oscillator strength at a particular wavelength *i* within 200 – 800 nm range. f_θ denotes the average value of oscillator strengths for a particular molecular conformation. For others without *meso*-aryl substitution, the LHE values were obtained according to Equation (2) (Sanusi *et al.*, 2023):

$$LHE = 1 - 10^{-(\Sigma_{i=1}^{N} f_i)/N} \qquad (2)$$

Note that Eq. (1) is new, and it is an improvement on Eq. (2) to incorporate the effect of dihedral rotation on the electronic spectra of the porphyrins. The dihedral rotation was introduced to account for the increase in the number of degrees of freedom in *meso*-aryl porphyrins compared to those without *meso*-aryl substituents.

Table 1 shows the LHE values obtained for all the investigated molecules in vacuum and in each of the selected solvent media. Generally, the LHE values were found to be in the range 0.11 – 0.24 in all the solvents with the highest value found to be exhibited by Por7 (0.24) in AcCN, DMSO and EtOH. The DCM value (0.23) of the compound is also close to the value obtained in the other three solvents. LHE is the ability of a molecule to harvest a substantial amount of incident light directed to it. It is a ground state electronic property of the dye and as the name suggests, it is a measure of the light harvesting efficiency, describing the light absorbing ability as a percentage.

Table 1: Calculated LHE and ϕ_f of all studied molecules in the selected solvent media.

Sample	**AcCN**		**DCM**		**DMSO**		**EtOH**		**Vac**	
	LHE	ϕ_f	**LHE**	ϕ_f	**LHE**	ϕ_f	**LHE**	ϕ_f	**LHE**	ϕ_f
Por1	0.21	0.42	0.20	0.42	0.21	0.42	0.21	0.42	0.15	0.31
Por2	0.20	0.59	0.20	0.05	0.20	0.51	0.20	0.59	0.15	0.41
Por3	0.21	0.48	0.20	0.42	0.21	0.43	0.21	0.43	0.16	0.35
Por4	0.23	0.48	0.22	0.53	0.23	0.55	0.23	0.53	0.16	0.38
Por5	0.21	0.53	0.21	0.55	0.21	0.60	0.21	0.43	0.16	0.47
Por6	0.23	0.48	0.22	0.48	0.23	0.54	0.22	0.48	0.16	0.43
Por7	0.24	0.37	0.23	0.27	0.24	0.31	0.24	0.27	0.17	0.33
Por8	0.19	0.32	0.19	0.31	0.19	0.27	0.19	0.32	0.17	0.28
Por9	0.23	0.22	0.22	0.28	0.23	0.28	0.23	0.25	0.18	0.19
Por10	0.16	0.29	0.16	0.29	0.16	0.29	0.16	0.29	0.14	0.25
Por11	0.17	0.29	0.17	0.29	0.17	0.29	0.17	0.29	0.14	0.25
Por12	0.17	0.29	0.18	0.29	0.18	0.29	0.17	0.29	0.15	0.25
Por13	0.11	0.23	0.23	0.22	0.23	0.34	0.23	0.34	0.18	0.30
Por14	0.11	0.36	0.22	0.37	0.22	0.37	0.22	0.37	0.10	0.29
Pht1	0.09	0.40	0.09	0.09	0.12	0.13	0.09	0.33	0.06	0.16
Pht2	0.21	0.05	0.21	0.06	0.21	0.11	0.21	0.01	0.19	0.14
Pht3	0.20	0.09	0.21	0.09	0.20	0.10	0.20	0.08	0.19	0.14
Pht4	0.11	0.18	0.17	0.03	0.12	0.14	0.12	0.15	0.19	0.10
Pht5	0.22	0.09	0.22	0.09	0.22	0.09	0.22	0.08	0.20	0.07
Pht6	0.21	0.08	0.22	0.09	0.22	0.09	0.21	0.07	0.20	0.07
Pht7	0.21	0.09	0.22	0.08	0.22	0.09	0.21	0.09	0.21	0.07

It thus means that for a full AM 1.5 light directed at the compounds studied here, only Por7 would have the capacity to harvest up to 24%. Structurally, Por7 is crowdedly decorated by -NH_2 group which could act as an effective light absorbing chromophore than the -COOH group which decorate most of the other investigated compounds. The LHE value of Por7 in vacuum was 0.17, a median range value relative to the highest (0.21) and the lowest (0.10) LHEs recorded for Pht7 and Por14, respectively (Table 1). This observation indicates that there is a strong contribution from the solvents to the LHE values of Por7. However, for Pht7, the values in the four solvents toggle between 0.21 and 0.22, indicating that there is no appreciable solvent effect on its LHE value in solvents relative to the vacuum. It is noteworthy that a high LHE value does not necessarily translate to a high electron injection rate or high photovoltaic efficiency. This is because the latter two parameters depend on the excited state properties of the sensitizer (Sanusi *et al*., 2019; Sanusi *et al*., 2020).

The fluorescence factor (ϕ_f) has been adopted as the approximate electron injection efficiency of the sensitizers (Sanusi *et al*., 2019; Sanusi *et al*., 2020). It is estimated by finding the ratio of the area under the computed emission to that of the computed absorption curves of the sensitizer (Sanusi *et al*., 2019; Sanusi *et al*., 2020). It measures the relative number of electrons injected from the excited dye molecules into the TiO_2 conduction band (Sanusi *et al*., 2019; Sanusi *et al*., 2020). The highest values were found for Por2 and Por5 (Table 1). Por5 ϕ_f in DCM, DMSO and vacuum are respectively 0.55, 0.60 and 0.47. No other molecules among those considered here surpassed Por5 in ϕ_f value in these three media. The presence of alkynyl group without any electron withdrawing group around it as found in others with a similar alkynyl group may be responsible for the high ϕ_f recorded in Por5. But for Por2, the same high value (0.59) was recorded in the two solvents, AcCN and EtOH.

For the electron injection process to be thermodynamically feasible, the CB edge of TiO_2 must be positioned below the LUMO level of the sensitizer (Sanusi *et al*., 2019; Sanusi *et al*., 2020). That is, the energy difference between the LUMO level and the CB edge of TiO_2 (δ_p) must be positive (Sanusi *et al*., 2019; Sanusi *et al*., 2020; Balanay and Kim, 2008). The optimum value of the potential gap (δ_p) has been estimated to be ~0.40 eV (Sanusi *et al*., 2019; Sanusi *et al*., 2020; Balanay and Kim, 2008; Mosurkal *et al*., 2005).

All the studied porphyrinoids showed positive δ_p values in the selected media except Pht2, Pht3, Pht4, Pht5, Pht6 and Pht7 in DCM and vacuum phases, which have negative δ_p values. The negative δ_p values imply that the transmission of electrons from the excited LUMO state of the porphyrinoids to the CB edge of the TiO_2 semiconductor in the affected media would be non-spontaneous (thermodynamically unfavorable). This particular set of compounds however showed the most interesting δ_p values in AcCN, DMSO and EtOH where their values are close to the optimal range of 0.40 – 0.45 eV (Balanay and Kim, 2008; Mosurkal *et al*., 2005), Table 2. The electron transmission from the excited LUMO state of these compounds to the CB edge of the TiO_2 semiconductor in the solvents would be expectedly spontaneous with their overall electron injection rate and photovoltaic efficiency sufficiently enhanced. Other compounds (Por1 – Por14, and Pht1) with relatively high but positive δ_p values even though would show spontaneous electron transmission, their injection rate to the CB edge of TiO_2 may be slow.

The charge collection efficiency (η_c) values (Table 3) obtained for Pht2, Pht3, Pht4, Pht5, Pht6 and Pht7 in DCM and in vacuum are imaginary values, since their δ_p values in these media are negative. The higher the η_c, the higher the rate of charge transport in the TiO_2 semiconductor (Sanusi *et al*., 2019; Sanusi *et al*., 2020). As expected and based on the closeness of δ_p values to the optimal δ_p values, the η_c of Pht2 – Pht7 in AcCN and EtOH are mostly favoured (Table 3). However, the η_c of this same set of compounds (Pht2 – Pht7) in DMSO was so unexpectedly low, even though their δ_p values are closed to the optimal value too. This behaviour may be attributed to the high viscosity of DMSO which slows down the velocity of their charges in this solvent.

The incident-photon conversion efficiency (IPCE), a function of the LHE, ϕ_f, and η_c measures the overall photovoltaic performance of the sensitizer (Sanusi *et al*., 2019; Sanusi *et al*., 2020). The highest performing sensitizer and the best solvent media for photovoltaic activity are provided in Table 2.

The best performing sensitizers in the order of decreasing IPCE values are Por2 > Pht7 > Pht4 > Por6 > Pht3 > Por4 in AcCN as the solvent. Only Por6 in DCM recorded a relatively high IPCE value of 5.05×10^{-11}. The values in red under DCM and vacuum are imaginary as foisted by the positions of their LUMOs which were found to be unaligned with the CB edge of the TiO_2 semiconductor. The IPCE values in DMSO and EtOH were incredibly low, and the reasons have been previously attributed to a possible enveloping bond formed between the O atoms of the solvents (DMSO and EtOH), and the Ti^{4+} of the TiO_2 semiconductor (Sanusi *et al*., 2023). A further decrease in IPCE of the compounds in DMSO was observed relative to the values in EtOH, and which has been assumed to be due to the inhibiting effect of viscosity on the charges' motion in DMSO (Sanusi *et al*., 2023). This study predicts that Por2 and Pht7 are the best sensitizers among those investigated. It also shows the enduring property of AcCN as the most suitable solvent for photovoltaic activity.

Table 2: The estimated δp and IPCE values of all studied molecule in vacuum and the selected solvents.

Sample	**AcCN**		**DCM**		**DMSO**		**EtOH**		**Vac**	
	δ_p	**IPCE × 10^{-11}**	**δ_p**	**IPCE × 10^{-11}**	**δ_p**	**IPCE × 10^{-11}**	**δ_p**	**IPCE × 10^{-11}**	**δ_p**	**IPCE × 10^{-11}**
Por1	1.52	3.09	1.63	2.56	1.50	0.61	1.53	0.99	2.14	1.70
Por2	1.22	6.85	1.35	0.45	1.21	1.16	1.24	2.19	2.02	2.57
Por3	1.53	3.67	1.64	2.70	1.52	0.64	1.55	1.04	2.17	2.00
Por4	1.35	5.06	1.44	4.69	1.34	1.12	1.37	1.80	1.91	2.90
Por5	1.43	4.80	1.49	4.40	1.43	1.06	1.44	1.27	1.72	4.35
Por6	1.27	5.79	1.32	5.05	1.27	1.26	1.28	1.84	1.51	5.22
Por7	1.70	2.78	1.79	1.73	1.69	0.45	1.71	0.66	2.23	2.05
Por8	1.74	1.84	1.80	1.66	1.73	0.31	1.75	0.60	2.12	1.91
Por9	1.21	2.95	1.23	3.57	1.20	0.75	1.21	1.11	1.28	3.41
Por10	1.75	1.30	1.80	1.24	1.74	0.26	1.76	0.43	2.00	1.51
Por11	1.70	1.38	1.74	1.33	1.70	0.27	1.71	0.45	1.89	1.72
Por12	1.63	1.54	1.65	1.51	1.63	0.30	1.63	0.51	1.67	2.21
Por13	1.38	1.14	1.44	2.06	1.38	0.67	1.39	1.20	1.74	3.04
Por14	1.36	1.87	1.41	3.39	1.35	0.73	1.37	1.22	1.62	1.80
Pht1	1.56	0.97	2.29	0.10	1.50	0.08	1.66	0.23	11.5	0.01
Pht2	0.57	2.31	**-0.39**[*]	5.73	0.65	0.73	0.42	0.15	**-11.1**[*]	0.03
Pht3	0.50	5.13	**-0.44**[*]	6.82	0.58	0.80	0.37	2.84	**-11.0**[*]	0.03
Pht4	0.46	6.32	**-0.47**[*]	1.35	0.54	0.72	0.32	3.72	**-10.9**[*]	0.02
Pht5	0.55	4.54	**-0.41**[*]	8.10	0.63	0.66	0.41	2.44	**-11.0**[*]	0.02
Pht6	0.53	4.31	**-0.45**[*]	6.58	0.59	0.74	0.38	2.39	**-11.0**[*]	0.02
Pht7	0.44	6.63	**-0.54**[*]	4.01	0.52	0.90	0.29	4.96	**-11.1**[*]	0.02

[*] IPCE values are imaginary.

Table 3: Estimated charge collection efficiency (η_c) values of all studied molecule in vacuum and the selected solvents.

Sample	**$\eta_c \times 10^{-10}$**				
	AcCN	**DCM**	**DMSO**	**EtOH**	**Vac**
Por1	3.57	3.08	0.70	1.16	3.60
Por2	5.67	4.60	1.11	1.82	4.12
Por3	3.63	3.14	0.71	1.17	3.61
Por4	4.60	4.01	0.90	1.49	4.60
Por5	4.25	3.93	0.82	1.39	5.90
Por6	5.24	4.86	1.02	1.71	7.46
Por7	3.15	2.84	0.61	1.03	3.60
Por8	2.98	2.76	0.58	0.97	3.97
Por9	5.93	5.67	1.15	1.95	10.41
Por10	2.79	2.60	0.54	0.92	4.22
Por11	2.90	2.80	0.56	0.95	4.70
Por12	3.10	3.00	0.60	1.02	5.88
Por13	4.41	4.07	0.86	1.44	5.60
Por14	4.54	4.21	0.88	1.48	6.30
Pht1	2.62	1.20	0.55	0.76	0.10
Pht2	21.51	**45.66***	3.21	13.13	**0.12***
Pht3	27.40	**36.50***	3.93	17.30	**0.11***
Pht4	31.28	**29.62***	4.44	21.51	**0.11***
Pht5	22.99	**41.48***	3.39	13.92	**0.12***
Pht6	25.11	**33.99***	3.88	15.80	**0.11***
Pht7	34.78	**23.06***	4.78	25.92	**0.11***

*Charge collection efficiency (η_c) values are imaginary.

Presented in Table 4 are the comparative photovoltaic performance of the best of the studied molecules and those that have been previously reported by our group. IPCE values being the overall photovoltaic efficiency parameter is used as the basis of comparison. We chose to limit this comparison to the reported works of this group because of lack of uniform computable photovoltaic efficiency parameters acceptable to all researchers. There are a wide range of different parameters that researchers often use as standard to describe the overall photovoltaic performance of dyes. Parameters such as LUMO-HOMO gaps, δ_p and η_c values, Φ_{inj}, and LHE, which separately and independently contribute to the overall photovoltaic efficiency of dyes are being used. But for us as a group, we believe the IPCE stands the greatest chance of giving the most accurate description of the overall photovoltaic performance of sensitizers, because it is a function of LHE, Φ_{inj} and η_c, while the η_c is also a function of δ_p. The IPCE aggregates the effect of each of these parameters to predict the overall photovoltaic performance of sensitizers. It is based on this justifiable reason that it is considered most appropriate as overall photovoltaic efficiency descriptor.

In Table 4, the vacuum performance of the porphyrins that have been investigated showed that the asymmetric molecule F with a central ruthenium metal and a single -CO_2H group as one of the substituents (Sanusi *et al*., 2019), is the best. For the phthalocyanines, it was found that molecule 8 (Sanusi *et al*., 2020) with a central ruthenium ion gave the highest IPCE value so far. This underscores the important role of ruthenium metal as central ion in dyes for DSSC. The solution phase performance indicates that Por2 in the current study, and molecule 5, an iron(II) phthalocyanine (Sanusi *et al*., 2020), both in AcCN gave the highest IPCE value in solution. The result in solution phase underscores the enduring property of AcCN as the most suitable solvent for photovoltaic activity.

Table 4: Overview of IPCE values of previously investigated porphyrinoids in vacuum, dichloromethane (DCM) and acetonitrile (AcCN) with references.

Pseudo-name	Porphyrinoid type		Porphyrinoid type		Porphyrinoid type	
	Porphyrin (vacuum)	Phthalocyanine (vacuum)	Porphyrin (DCM)	Phthalocyanine (DCM)	Porphyrin (AcCN)	Phthalocyanine (AcCN)
F (Sanusi *et al*., 2019)	4.82×10^{-10}	-	NA	-	NA	-
C (Sanusi *et al*., 2023)	0.290×10^{-10}	-	0.30×10^{-10}	-	0.330×10^{-10}	-
5 (Sanusi *et al*., 2020)	-	0.110×10^{-10}	-	NA	-	12.1×10^{-10}
6 (Sanusi *et al*., 2023)	0.0450×10^{-10}	-	0.041×10^{-10}		0.0390×10^{-10}	-
8 (Sanusi *et al*., 2020)	-	1.73×10^{-10}	-	NA	-	0.280×10^{-10}
Por2*	0.257×10^{-10}	-	0.045×10^{-10}	-	0.685×10^{-10}	-
Pht7*	-	Im	-	Im	-	0.663×10^{-10}

*This study. Im = imaginary value.

CONCLUSION

Effects of substituents and solvents on the photovoltaic properties of some selected porphyrinoid compounds as sensitizers in dye-sensitized solar cells (DSSCs) have been investigated. The photophysical and photovoltaic properties of these compounds were studied in vacuum, acetonitrile (AcCN), dichloromethane (DCM), dimethyl sulfoxide (DMSO), and ethanol (EtOH). The best performing sensitizers judging by their IPCE values were found to be Por2 (6.85×10^{-11}) and Pht7 (6.63×10^{-11}) with AcCN as the solvent. The compounds did not show considerable photovoltaic performance in the other solvents (DCM, DMSO and EtOH). Overall, the study predicts that Por2 and Pht7 are the best sensitizers among those investigated. It also shows the enduring property of AcCN as the most suitable solvent for photovoltaic activity.

ACKNOWLEDGEMENT

KS and NOF are grateful to Dr. P. B. Khoza and the management of the Centre for High Performance Computing (CHPC), South Africa, for access to their central supercomputing cluster.

REFERENCES

Andrade, S. M., Teixeira, R., Costa, S. M. B., and Sobral, A. J. F. N. (2008). Self-aggregation of free base porphyrins in aqueous solution and in DMPC vesicles. *Biophysical Chemistry*, 133(1-3), 1 – 10.

Balanay, M. P. and Kim, D. H. (2008). DFT/TD-DFT molecular design of porphyrin analogues for use in dye-sensitized solar cells, *Physical Chemistry Chemical Physics*, 10, 5121 – 5127.

Carella, A., Borbone, F. and Centore, R. (2018). Research progress on photosensitizers for DSSC. *Frontiers in Chemistry*, 6, 481-505.

Ding, X., Wei, S., Bian, H., Zhu, L., and Xia D. (2021). Insights into the self-aggregation of porphyrins and their influence on asphaltene aggregation. *Energy and Fuels*, 35(15), 11848 – 11857.

Desai, J. and Nelson, M. (2017). Are we headed for a solar waste crisis? *Environmental Progress and Sustainable Energy*, 36(4), 1047–1050.

Devadiga, D., Selvakumar, M., Shetty, P. and Santosh, M. S. (2021). Dye-sensitized solar cell for indoor applications: A mini-review. *Journal of Electronic Material*, 50, 3187–3206.

Ellis, H. (2014). Characterization of dye-sensitized solar cells: Components for environment friendly photovoltaics [Licentiate dissertation]. Uppsala University.

Gerischer, H. (1968). The influence of the semiconductor structure on the kinetics of photoelectrochemical reactions. *Journal of Electroanalytical Chemistry*, 20, 12-25.

Green, M. A., Hishikawa, Y., Dunlop, E. D., Levi, D. H., Hohl-Ebinger, J., and Ho-Baillie, A. W. Y. (2018). Solar cell efficiency tables (version 51). *Progress in Photovoltaics: Research and Applications*, 26(1), 3–12.

High, J. S., Virgil, K. A., and Jakubikova, E. (2015). Electronic Structure and Absorption Properties of Strongly Coupled Porphyrin−Perylene Arrays. *Journal of Physical Chemistry A*, 119, 9879-9888.

International Energy Agency. (2020). World energy outlook 2020. https://www.iea.org/reports/world-energy-outlook-2020

Kadish, K. M., Smith, K. M., and Guilard, R. (Eds.). (2019). The porphyrin handbook: Phthalocyanines: Properties and materials (Vol. 23). Academic Press.

Kaliramna, S., Dhayal, S. S., Chaudhary, R., Khaturia, S., Ameta, K. L., and Kumar, N. (2022). A review and comparative analysis of different types of dyes for applications in dye-sensitized solar cells. *Brazilian Journal of Physics*, 52, 136.

Labella, J. and Torres, T. (2023). Subphthalocyanines: contracted porphyrinoids with expanded applications. *Trends in Chemistry*, 5(5), 353-366.

Li, H., Jensen, T. J., Fronczek, F. R., and Vicente M. H. (2008). Syntheses and properties of a series of cationic water-soluble phthalocyanines. *Journal of Medicinal Chemistry*, 51(3), 502-511.

Liu, W., Jensen, T. J., Fronczek, F. R., Hammer, R. P., Smith, K. M., and Vicente, M. H. (2005). Synthesis and cellular studies of non-aggregated water-soluble phthalocyanines. *Journal of Medicinal Chemistry*, 48(4), 1033-1041.

Lu, J., Liu, S., and Wang, M. (2018). Push-pull zinc porphyrins as light-harvesters for efficient dye-sensitized solar cells. *Frontiers* in *Chemistry*, 6: 541.
doi: 10.3389/fchem.2018.00541.

Matsuo, Y., Ogumi, K., Jeon I., Wang, H., and Nakagawa, T. (2020). Recent progress in porphyrin- and phthalocyanine containing perovskite solar cells. *RSC Advances*, 10, 32678-32689.

Mehmood, U., Rehman, S., Harrabi, K., Hussein, I.A., and Reddy, B. V. S. (2014). Recent advances in dye sensitized solar cells. *Advances in Materials Science and Engineering* 974782, 1–12.

Mohamed, Y., Asmae, B., Cemi, O., Zeynel, S., and Mika, S. (2021). Organic/metal-organic photosensitizers for dye-sensitized solar cells (DSSC): Recent developments, new trends, and future perceptions. *Dyes Pigments*, 192, 109227.

Mosurkal, R., Kumar, R., Bruno, F. F., Nagarajan, R., Samuelson, L. and Kumar, J. (2005). Biocatalytic synthesis of novel electronic and photovoltaic materials. *Pure Applied Chemistry*, 77(1), 263 – 272.

O’Regan, B. and Grätzel, M. (1991). A low-cost, high-efficiency solar cell based on dye-sensitized colloidal TiO2 films. *Nat*ure, 353(6346), 737-740.

Pashaei, B., Shahroosvand, H., and Abbasi, P. (2015). Transition metal complex redox shuttles for dye-sensitized solar cells. *RSC Advances*, 5(97), 79874–79893.

Prathapan, S., Johnson, T. E., and Lindsey, J. S. (1993). Building-block synthesis of porphyrin light-harvesting arrays. *Journal of America Chemical Society*, 115 (16), 7519 – 7520.

Safar-Sajadi, S. M., Khoee, S. (2021). The simultaneous role of porphyrins’ H- and J- aggregates and host-guest chemistry on the fabrication of reversible Dextran-PMMA polymersome. *Scientific Report*, 11(2832).
doi.org/10.1038/s41598-021-82256-7.

Sanusi, K., Amuhaya, E. K., and Nyokong, T. (2014a). Enhanced optical limiting behavior of an indium phthalocyanine-single-walled carbon nanotube composite: an investigation of the effect of solvents. *Journal Physical Chemistry C*, 118, 7057 – 7069.

Sanusi, K., Antunes, E., and Nyokong, T. (2014b). Optical nonlinearities in non-peripherally substituted pyridyloxy phthalocyanines: a combined effect of symmetry, ring-strain and demetallation. *Dalton Transactions*, 43, 999 – 1010.

Sanusi, K., Atewolara-Odule, O. C., Sanyaolu, N. O., Ibikunle, A. A., Khoza, P. B., Fatomi, N. O., Fasanya, S. A., Abuka, H. E., Jesugbile, E. O., Yilmaz, Y., and Ceylan, Ü. (2023). Effects of solvents and substituents on the adsorptive and photovoltaic properties of porphyrins for dye-sensitized solar cell application: a theoretical consideration. *Structural Chemistry*, 34, 891–904.

Sanusi, K., Ceylan, Ü., Yilmaz, Y., and George, R. C. (2020). A DFT/TD-DFT study on the possible replacement of Ru(II) with Fe(II) in phthalocyanine-based dye-sensitized solar cells. *Structural Chemistry*, 31, 2301–2311.

Sanusi, K., Fatomi, N. O., Aderogba, A. A., Khoza, P. B., and Igumbor, E. (2023). A DFT study of solvent and substituent effects on the adsorptive and photovoltaic properties of some selected porphyrin derivatives for DSSC application. *Journal of Fluorescence*
doi.org/10.1007/s10895-023-03447-1.

Sanusi, K., Fatomi, N. O., Borisade, A. O., Yilmaz, Y., Ceylan, Ü., and Fashina, A. (2019). An approximate procedure for profiling dye molecules with potentials as sensitizers in solar cell application: A DFT/TD-DFT approach. *Chem*ical *Phys*ics *Lett*ers, 722, 1–8.

Sanusi, S. O., Antunes, E., and Nyokong, T. (2013). Nonlinear optical behavior of metal octaphenoxy phthalocyanines: effect of distortion caused by the central metal. *Journal of Porphyr*ins and *Phthalocya*nines, 17, 920 – 927.

Shockley, W. and Queisser, H. J. (1961). Detailed balance limit of efficiency of p-n junction solar cells. *Journal of Applied Physics*, 32(3), 510–519.

Singh, A. Singh, A. K., Dixit, R., Vanka, K., Krishnamoorthy, K., and Nithyanandhan, J. (2023). Visible-light-active unsymmetrical squaraine dyes with 1 V of open-circuit voltage for dye-sensitized solar cells. *ChemPhotoChem*, doi.org/10.1002/cptc.202200328.

Spinelli, G., Freitag, M. and Benesperi, I. (2023). What is necessary to fill the technological gap to design sustainable dye-sensitized solar cells? *Sustainable Energy and Fuels*, 7, 916–927.

Tavakoli, E., Kakekhani, A., Kaviani, S., Tan, P., Ghaleni, M. M., Zaeem, M. A., Rappe, A. M., and Nejati, S. (2019). *In Situ* Bottom-up synthesis of porphyrin-based covalent organic frameworks. *Journal of America Chemical Society*, 141 (50), 19560 – 19564.

Thanthiriwatte, K. S. and de Silva, K. M. N. (2002). Non-linear optical properties of novel fluorenyl derivatives - ab initio quantum chemical calculations. *Journal of Molecular Structure: THEOCHEM.*, 617(1-3), 169–175.

Tomasi, J., Mennucci, B., Cammi, R. (2005). Quantum mechanical continuum solvation models. *Chemistry Review*, 105, 2999–3093.

Tontapha, S., Sang–aroon, W., Kanokmedhakul, S., Promgool, T., and Amornkitbamrung, V. (2017). Effects of dye-adsorption solvents, acidification and dye combination on efficiency of DSSCs sensitized by α-mangostin and anthocyanin from mangosteen pericarp. *J. Materials Science: Mate*rials in *Electronics*, 28, 7454–7467.

Urbani, M., Ragoussi, M-E., Nazeeruddin, M. K., and Torres, T. (2019). Phthalocyanines for dye-sensitized solar cells. *Coordination Chemistry Review*, 381, 1 – 64.

Wang, H., Cobb, B., van Breemen, A., Gelinck, G., and Bao, Z. (2014). A fast and robust method to achieve high-performance flexible organic field-effect transistors. *Advanced Materials*, 26(28), 4588-4593.

Xu, R., Yang, L., Yang, B., Wang, W., Yao, Q., Li, J., Liu, X., Chen, P. and Peng, X. (2023). An integrated design strategy of zinc phthalocyanine dyes for LCD dye-based color filters. *Dyes Pigments*, 219, 111562.

Yilmaz, Y., Özdemir, M., Sanusi, K., Fatomi, O. Nafisat, Khoza, P. B. (2022). Aggregation effect on phthalocyanine photocatalytic degradation efficiency using orange G and methyl orange as test-pollutant compounds in aqueous medium. *ChemistrySelect*, 7, e2022202958, 1 -10. doi.org/10.1002/slct.202202958.